

Electric-Octupole and Pure-Electric-Quadrupole Effects in Soft-X-Ray Photoemission

A. Derevianko,^{1,*} O. Hemmers,² S. Oblad,² P. Glans,³ H. Wang,⁴ S. B. Whitfield,⁵ R. Wehlitz,⁶ I. A. Sellin,⁷
W. R. Johnson,¹ and D. W. Lindle²

¹*Department of Physics, University of Notre Dame, Notre Dame, Indiana 46556*

²*Department of Chemistry, University of Nevada, Las Vegas, Nevada 89154-4003*

³*Atomic Physics, Stockholm University, 10405 Stockholm, Sweden*

⁴*Department of Physics, Uppsala University, Box 530, S-751 21 Uppsala, Sweden*

⁵*Department of Physics, University of Wisconsin, Eau Claire, Wisconsin 54702*

⁶*Synchrotron Radiation Center, University of Wisconsin, Stoughton, Wisconsin 53589*

⁷*Department of Physics, University of Tennessee, Knoxville, Tennessee 37996*

(Received 11 August 1999)

Second-order [$O(k^2)$, $k = \omega/c$] nondipole effects in soft-x-ray photoemission are demonstrated via an experimental and a theoretical study of angular distributions of neon valence photoelectrons in the 100–1200 eV photon-energy range. A newly derived theoretical expression for nondipolar angular distributions characterizes the second-order effects using four new parameters with primary contributions from pure-quadrupole and octupole-dipole interference terms. Independent-particle calculations of these parameters account for a significant portion of the existing discrepancy between experiment and theory for Ne $2p$ first-order nondipole parameters.

PACS numbers: 32.80.Fb, 31.25.Eb, 32.30.Rj

A mainstay of photoemission is the (electric-)dipole approximation (DA), in which all higher-order multipoles are neglected [1]. The range of validity of the DA received renewed interest as recent experiments [2–4] uncovered breakdowns at progressively lower photon energies. At high energies ($\hbar\omega > 5$ keV), breakdown of the DA in photoionization is well known, and a proper description requires inclusion of many multipoles [5]. For soft-x-ray ($\hbar\omega < 5$ keV) photoionization, in contrast, first-order [$O(k)$] corrections to the DA generally have been considered sufficient [6]. At these relatively low energies, DA breakdown primarily leads to forward/backward asymmetries in photoelectron angular-distribution patterns. Especially striking have been observations [3,4] and predictions [7] of nondipole effects at energies well below 1 keV, a region in which the DA is usually considered valid. In the present work, experimental and theoretical analysis of neon valence photoemission demonstrates a new, and unexpected, breakdown: significant second-order [$O(k^2)$] nondipole effects, primarily due to electric-octupole and pure-electric-quadrupole interactions, in low-energy photoemission.

We begin with Cooper's [8] $O(k)$ formula for the differential photoionization cross section of subshell (n, κ) in a randomly oriented target using linearly polarized light:

$$\frac{d\sigma_{n\kappa}}{d\Omega} = \frac{\sigma_{n\kappa}}{4\pi} \{1 + \beta_{n\kappa} P_2(\cos\theta) + (\delta_{n\kappa} + \gamma_{n\kappa} \cos^2\theta) \sin\theta \cos\phi\}, \quad (1)$$

where $\sigma_{n\kappa}$ is the photoionization cross section, $\beta_{n\kappa}$ describes the angular distribution within the DA, and $\delta_{n\kappa}$ and $\gamma_{n\kappa}$ are nondipole angular-distribution parameters characterizing the leading first-order corrections to the DA

(mostly $E_2 - E_1$ terms). The angles θ and ϕ are determined by the direction of the photoelectron relative to the photon-polarization $\hat{\epsilon}$ and photon-propagation \mathbf{k} directions, respectively. The first two terms on the right of Eq. (1) constitute the usual DA expression for the differential cross section, and the DA notion of a "magic angle" [$\theta_m = 54.7^\circ$, $P_2(\cos\theta_m) = 0$] is preserved only in the $\phi = 90^\circ$ plane perpendicular to \mathbf{k} .

Interpreted at this level of approximation, recent rare-gas experiments [2,3] observed significant modifications of photoelectron angular distributions from DA expectations, generally in good agreement with first-order independent-particle-approximation (IPA) calculations [8,9]. The only exception is Ne $2p$ [3]; while measured values of γ_{2s} (δ_{2s} is negligible when $\beta_{2s} = 2$) agree with theory, measured values of the combined parameter ζ_{2p} ($= 3\delta_{2p} + \gamma_{2p}$) are 30% larger than IPA predictions for energies near 1 keV.

The same experiment found β_{2p} also disagrees substantially with IPA calculations in this energy region but is in close agreement with correlated calculations using the random-phase approximation (RPA) [10,11], thereby identifying important electron-correlation effects well above the $n = 2$ thresholds [12]. This result led to speculation [3] that the discrepancy between measured and IPA-calculated ζ_{2p} values might also be due to interchannel-coupling effects. However, subsequent first-order nondipole calculations including correlation [13] disproved this notion; RPA values of Ne ζ_{2p} are in excellent agreement with uncorrelated IPA results [8,9].

In this work, we explain much of this discrepancy between theory and experiment for Ne ζ_{2p} . Beginning with theory, second-order [$O(k^2)$] corrections to the differential cross section, which arise from interferences between $E_1 - E_3$, $E_1 - M_2$, $E_2 - E_2$, $E_2 - M_1$, and $M_1 - M_1$,

and from retardation corrections to $E_1 - E_1$ amplitudes, are incorporated into Eq. (1):

$$\frac{d\sigma_{n\kappa}}{d\Omega} = \frac{\sigma_{n\kappa}}{4\pi} \{1 + (\beta_{n\kappa} + \Delta\beta_{n\kappa})P_2(\cos\theta) + (\delta_{n\kappa} + \gamma_{n\kappa} \cos^2\theta) \sin\theta \cos\phi + \eta_{n\kappa}P_2(\cos\theta) \cos 2\phi + \mu_{n\kappa} \cos 2\phi + \xi_{n\kappa}(1 + \cos 2\phi)P_4(\cos\theta)\}, \quad (2)$$

where the $O(k^2)$ parameters $\Delta\beta$, η , μ , and ξ are introduced [14]. Three of them satisfy the constraint $\eta + \mu + \xi = 0$. Reference [14] contains complete formulas and a tabulation of first- and second-order parameters for all subshells of the rare gases helium to xenon.

To obtain $O(k^2)$ predictions for comparison with experiment, we carried out numerical IPA studies of second-order corrections for neon. Wave functions for bound-state and continuum electrons were obtained from the radial Dirac equation in a modified Hartree potential. Values for all $n = 2$ angular-distribution parameters were calculated up to 2 keV. Our results for γ_{2s} and ζ_{2p} are in excellent agreement with previous nonrelativistic IPA calculations [8]. Figure 1 shows values for $\Delta\beta$, η , and μ ($\xi = -\eta - \mu$) obtained from our second-order IPA calculations. Primary contributions to these parameters come from $E_1 - E_3$ and $E_2 - E_2$ terms, with the octupole term contributing about 65% at 1 keV. A smaller contribution ($\approx 10\%$) comes from the $E_1 - M_2$ term.

The experiments were performed with four electron analyzers mounted in a chamber which can rotate about the photon beam [15]. At the nominal angular position of the apparatus, two analyzers are at θ_m and $\theta = 0^\circ$ in the plane perpendicular to the photon beam ($\phi = 90^\circ$), which we refer to as the dipole plane because first-order corrections vanish, while two more analyzers are positioned on the forward 35.3° cone with respect to the photon beam (see Fig. 2 inset for definition of angles). At the nominal position, these two “nondipole” analyzers are at $(\theta_m, \phi = 0^\circ)$

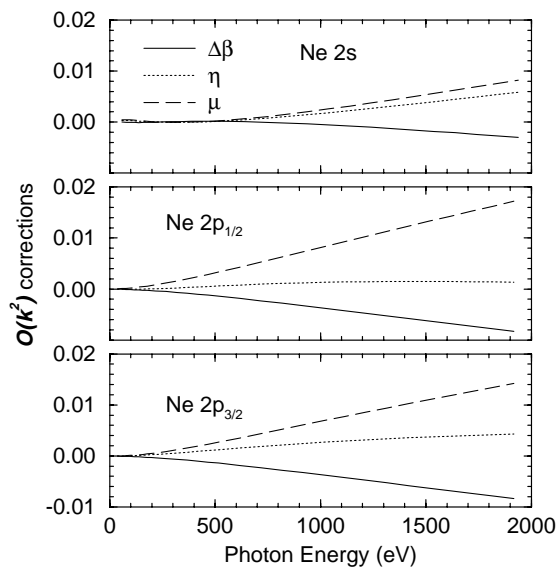


FIG. 1. Nondipole parameters of $O(k^2)$ for neon.

and ($\theta = 90^\circ$, $\phi = 35.3^\circ$). Photoemission intensities in the two magic-angle analyzers are independent of β and can differ only because of nondipole effects. While the magic angle is no longer strictly valid when second-order effects are included, calculations show they can be unimportant in certain geometries (see below).

We present experimental results for Ne γ_{2s} and ζ_{2p} , assuming the validity of Eq. (1), for comparison with $O(k)$ and $O(k^2)$ calculations. The first data set is based on angle-resolved photoemission intensities from the two magic-angle analyzers. Figure 2 compiles old [3] and new values for γ_{2s} and ζ_{2p} (open squares) determined using this geometry. The solid curves represent $O(k)$ calculations [8,9,13], which agree well with the $2s$ results but disagree with the $2p$ results above 800 eV.

For the magic-angle geometry, Eq. (2) and the results in Fig. 1 can be used to estimate $O(k^2)$ influences on the experimental determination of γ_{2s} and ζ_{2p} . For example, we predict measured values of ζ_{2p} will be perturbed by second-order effects as follows:

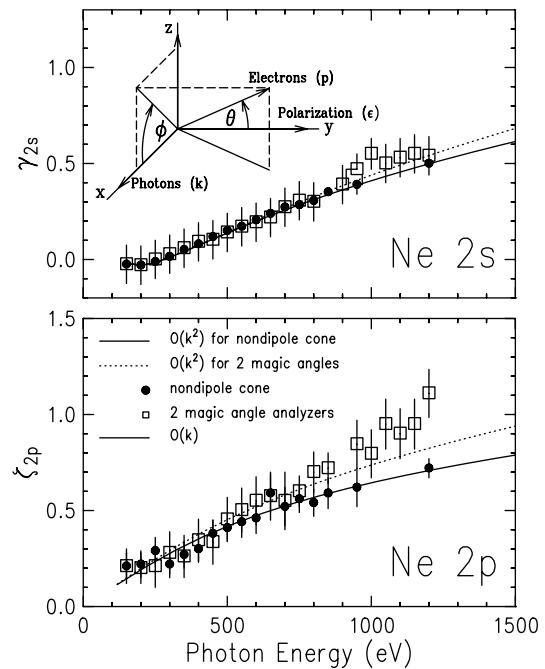


FIG. 2. Experimental and theoretical values of γ_{2s} and ζ_{2p} for neon determined under different geometrical conditions: (1) open squares and dotted curves relate to the magic-angle geometry; (2) solid circles and curves relate to the nondipole-cone geometry. Both dotted and solid curves include effects up to $O(k^2)$. The solid curves also represent first-order theory, independent of geometry. See text for complete description.

$$\zeta_{2p} = \sqrt{\frac{27}{2}} \left[\frac{\sigma(\theta_m, 0)}{\sigma(\theta_m, \pi/2)} - 1 \right] \quad (3)$$

$$\approx \frac{\gamma + 3\delta + \sqrt{54}(\mu - 7\xi/18)}{1 - \mu},$$

using the notation $\sigma(\theta, \phi) = \frac{d\sigma}{d\Omega}(\theta, \phi)$. From Eq. (3) and the results in Fig. 1, effective values for ζ_{2p} (and similarly γ_{2s}) have been determined, yielding the dotted curves in Fig. 2. We find excellent agreement for γ_{2s} and clearly improved agreement for ζ_{2p} . The second-order effects thus included account for much of the difference between first-order theory (solid curve) and experiment for ζ_{2p} , demonstrating the first observation of $O(k^2)$ effects in soft-x-ray photoemission.

To confirm this unexpected finding, new measurements in a different geometry were performed by rotating the apparatus to ten different angular positions about the photon beam, yielding 20 angle-resolved intensities for Ne 2s and 2p photoemission at different angles θ within the dipole plane, and 20 more at different angles θ and ϕ around the 35.3° nondipole cone. From the calculated results for $\Delta\beta_{2p}$ (Fig. 1), direct second-order effects on β_{2p} should be insignificant; $\Delta\beta_{2p} \approx 0.005$ near 1 keV, smaller than our measurement uncertainties. Therefore, values of β_{2p} determined from the dipole-plane spectra should agree well with DA calculations, if effects due to η , μ , and ξ are negligible in the dipole plane. In this plane, we predict their effects will mostly cancel, and thus the excellent agreement [12] between experiment and theory for β_{2p} is not surprising.

In the nondipole cone, however, influences of the $O(k^2)$ parameters are superimposed on intensity variations due to the dipole β and the $O(k)$ δ and γ parameters. But for both γ_{2s} and ζ_{2p} , our calculations predict effects due to η , μ , and ξ also mostly cancel in the nondipole-cone geometry, yielding the solid curves in Fig. 2. Furthermore, small residual effects around this cone are similar in sign and magnitude for 2s and 2p, which is relevant because 2s/2p intensity ratios are the raw input for data analysis. Assuming no influence of second-order effects in the nondipole cone, we modeled the measured ratios around this cone using Eq. (1) to derive values for γ_{2s} and ζ_{2p} . These results (solid circles in Fig. 2) agree extremely well with $O(k)$ calculations [8,9,13], confirming our prediction of near cancellation of $O(k^2)$ effects in this geometry.

The experimental geometries described above provide two independent methods to measure γ_{2s} and ζ_{2p} : one relying on measurements using the nondipole analyzers at many angles in the nondipole cone, the other relying on comparison between the (dipole and nondipole) magic-angle analyzers. For the former, we predict $O(k^2)$ effects mostly cancel. For the latter, in contrast, we expect the influences of η , μ , and ξ on Ne 2p photoemission to be opposite in sign for $\phi = 0^\circ$ and $\phi = 90^\circ$, because of

the $\cos(2\phi)$ terms in Eq. (2). Thus, second-order effects should be observable only in the latter geometry, hence the differences in measured values of ζ_{2p} shown in Fig. 2.

As a further demonstration of the influence of second-order nondipole effects on angle-resolved-photoemission intensities, Fig. 3 compares spectra taken with the two magic-angle analyzers. Figure 3a contains a neon photoemission spectrum taken at $\hbar\omega = 1200$ eV, θ_m , and $\phi = 90^\circ$ in the dipole plane, where influences of β , δ , and γ vanish. Included are fit curves showing modeled peak shapes and photoemission satellites to the left of the 2s peak. The overall fit (solid curve) matches the data very well, as indicated by the residual in Fig. 3b.

This spectrum and fit are reproduced in Fig. 3c and compared to a nondipole magic-angle spectrum at 1200 eV, θ_m , and $\phi = 0^\circ$. Intensity normalization between the spectra was achieved using γ_{2s} , for which experiment and theory agree well. By inspection, the 2s/2p ratio is different in the two spectra. One possible explanation is a differential influence of $O(k)$ nondipole effects on 2s and 2p intensities. As a quantitative test of this hypothesis, we derived the dotted region in Fig. 3c by multiplying the fit

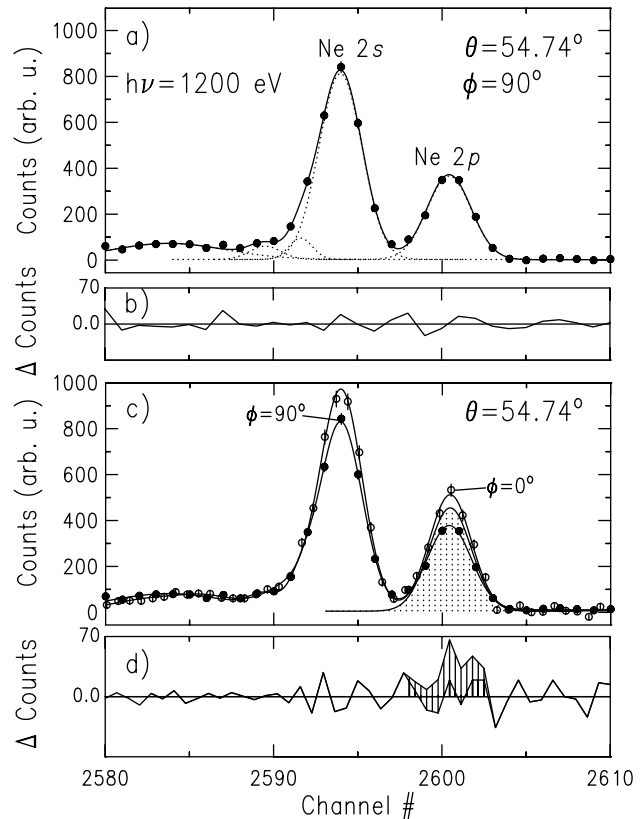


FIG. 3. Neon valence photoemission spectra at 1200 eV and $\theta_m = 54.7^\circ$. (a) $\phi = 90^\circ$ spectrum. (b) Residual of fit in (a). (c) Spectrum in (a) compared to a $\phi = 0^\circ$ spectrum. (d) Residual of fit to the $\phi = 0^\circ$ spectrum (lower curve), and difference between the $\phi = 0^\circ$ fit and the dotted region in (c) (upper curve). The hatched area in (d) is 2p photoemission intensity attributable to $O(k^2)$ corrections. See text for explanation.

to the $2p$ peak in the dipole magic-angle spectrum by the IPA-predicted differential effect on $2s$ and $2p$ peak intensities at the nondipole magic angle, which can be determined from the IPA-/RPA-predicted values for γ_{2s} and ζ_{2p} [see Eq. (1)]. If $O(k)$ effects alone explain the observed variation of the $2s/2p$ ratio between the two spectra, then the dotted region should coincide exactly with the $2p$ peak in the nondipole magic-angle spectrum. It does not, and the difference between the dotted region and the open-circle data ($\approx 10\%$) is attributed to the influence of second-order effects.

In conclusion, an experimental and theoretical study of neon valence photoemission has demonstrated the first observation of second-order (primarily $E_1 - E_3$ and $E_2 - E_2$) nondipole effects on photoelectron angular distributions in the soft-x-ray region. A general expression for the differential photoionization cross section, including all contributions through second order, has been derived in a form convenient for comparison to experiment.

This work was supported by NSF and DOE EPSCoR. A. D. and W. R. J. were supported in part by NSF Grant No. PHY-99-70666. D. W. L. acknowledges UNLV Sabbatical Leave support. Experiments performed at the Advanced Light Source (LBNL) were supported by DOE Materials Science Division, BES, OER under Contract No. DE-AC03-76SF00098.

*Present address: ITAMP, Harvard-Smithsonian Center for Astrophysics, Cambridge, MA 02138.

- [1] H. A. Bethe and E. E. Salpeter, *Quantum Mechanics of One- and Two-Electron Atoms* (Springer-Verlag, Berlin, 1957).
- [2] B. Krässig, M. Jung, D. S. Gemmell, E. P. Kanter, T. LeBrun, S. H. Southworth, and L. Young, Phys. Rev. Lett. **75**, 4736 (1995); M. Jung, B. Krässig, D. S. Gemmell, E. P. Kanter, T. LeBrun, S. H. Southworth, and L. Young, Phys. Rev. A **54**, 2127 (1996).
- [3] O. Hemmers, P. Glans, D. L. Hansen, H. Wang, S. B. Whitfield, D. W. Lindle, R. Wehlitz, J. C. Levin, I. A. Sellin, R. C. C. Perera, E. W. B. Dias, H. S. Chakraborty, P. C. Deshmukh, and S. T. Manson, J. Phys. B **30**, L727 (1997).
- [4] N. L. S. Martin, D. B. Thompson, R. P. Bauman, C. D. Caldwell, M. O. Krause, S. P. Frigo, and M. Wilson, Phys. Rev. Lett. **81**, 1199 (1998).
- [5] H. K. Tseng, R. H. Pratt, S. Yu, and A. Ron, Phys. Rev. A **17**, 1061 (1978).
- [6] D. W. Lindle and O. Hemmers, J. Electron Spectrosc. Relat. Phenom. **100**, 297 (1999), and references therein.
- [7] V. K. Dolmatov and S. T. Manson, Phys. Rev. Lett. **83**, 939 (1999).
- [8] J. W. Cooper, Phys. Rev. A **47**, 1841 (1993); **42**, 6942 (1990).
- [9] A. Bechler and R. H. Pratt, Phys. Rev. A **42**, 6400 (1990); **39**, 1774 (1989).
- [10] W. R. Johnson and C. D. Lin, Phys. Rev. A **20**, 964 (1979); W. R. Johnson and K. T. Cheng, *ibid.* **20**, 978 (1979).
- [11] M. Ya. Amusia and N. A. Cherepkov, *Case Studies in Atomic Physics* (North-Holland, Amsterdam, 1975), Vol. 5, p. 155.
- [12] E. W. B. Dias, H. S. Chakraborty, P. C. Deshmukh, S. T. Manson, O. Hemmers, P. Glans, D. L. Hansen, H. Wang, S. B. Whitfield, D. W. Lindle, R. Wehlitz, J. C. Levin, I. A. Sellin, and R. C. C. Perera, Phys. Rev. Lett. **78**, 4553 (1997).
- [13] W. R. Johnson, A. Derevianko, K. T. Cheng, V. K. Dolmatov, and S. T. Manson, Phys. Rev. A **59**, 3609 (1999).
- [14] A. Derevianko, W. R. Johnson, and K. T. Cheng, At. Data Nucl. Data Tables **73**, 153 (1999). The parameters λ and ν in this work are replaced here by η and ξ to avoid confusion with photon wavelength and frequency.
- [15] O. Hemmers, S. B. Whitfield, P. Glans, H. Wang, D. W. Lindle, R. Wehlitz, and I. A. Sellin, Rev. Sci. Instrum. **69**, 3809 (1998).